Journal of Materials Chemistry A

Accepted Manuscript

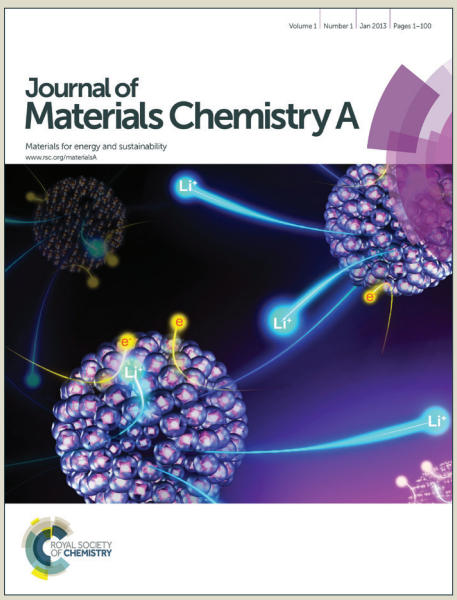

ROYAL SOCIETY OF CHEMISTRY

www.rsc.org/materialsA

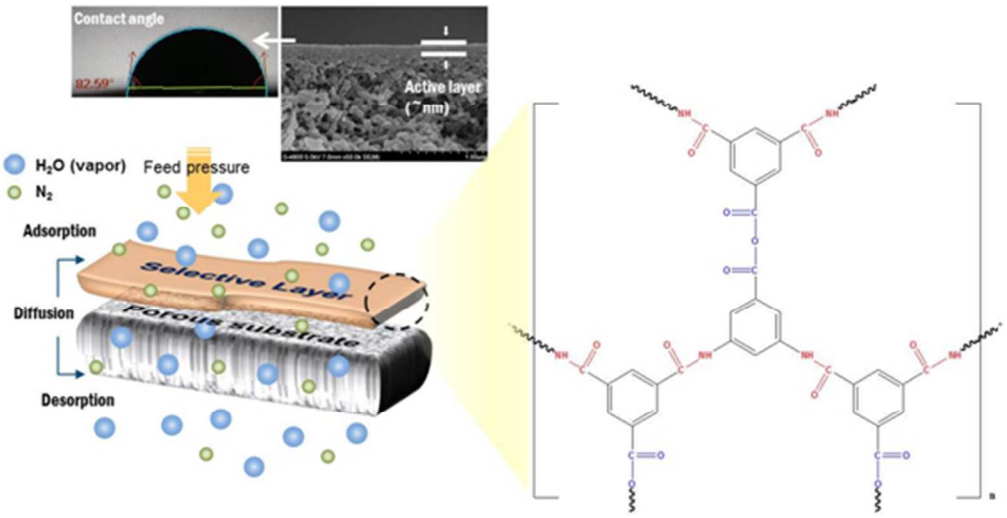

159x81mm (96 x 96 DPI)

Journal Name

RSCPublishing

ARTICLE

Synthesis of cross-linked amides and esters as thin film composite membrane materials yields permeable and selective for water vapor/gas separation

Cite this: DOI: 10.1039/x0xx00000x

Received 00th January 2012,
Accepted 00th January 2012

DOI: 10.1039/x0xx00000x

www.rsc.org/

Sang Hee Yun[a,b,†], Pravin G. Ingole[a,†], Won Kil Choi[a], Jong Hak Kim[b] and Hyung Keun Lee*[a]

In this work, 3,5-diaminobenzoic acid (BA) was selected to synthesize polyamide as a selective layer because it is considered desirable to fabricate hydrophilic thin film composite (TFC) membranes for water vapor separation. Cross-linked chains of TFC membranes by interfacial polymerization were suggested, confirmed and discussed by using the compiled results of characterization, such as ATR-FTIR, XPS, FE-SEM, and water contact angle. As a result, BA-1-10 membrane (1.0 wt. % of BA, 0.2 wt. % of TMC and 10 min of reaction time) showed the best permeance and separation factor as 2160 GPU and 23, respectively, compared with other TFC membranes prepared by different conditions. It was investigated that higher concentration of BA containing carboxylic acid is possible to diffuse faster, react more actively and form hydrophobic esters. Moreover, acyl chloride group (-COCl) of TMC was hydrolyzed to COOH and improved the hydrophilicity for better sorption of water vapor. However, the hydrophobic esters was generated on selective layer due to the excessive reaction time over 10 min. It was found that reaction time should be as same as immersion time of aqueous monomer to be adequate to high performances.

Journal Name RSCPublishing

ARTICLE

1. Introduction

Membrane separation has been utilized to improve the energy efficiency in separation process technologies for decades because separation process occurs under the law of thermodynamics and requires an amount of energy for operation.[1] Membrane technology is quietly desirable for separation process since it does not require phase change, consume a vast amount of additional energy, such as absorbents, or occupy the extensive operation site, leading to a potential of energy-efficient process.[2-4] In view of materials, the membranes can be largely classified into organic, inorganic and organic/inorganic hybrid according to their nature, geometry and separation regime.[5] Polymeric membranes as organic materials have been properly selected for major industrial applications such as reverse osmosis, pervaporation and gas separation etc.[2-6] and employ the solution-diffusion mechanism where the rate of each gas transport is related with the affinity between the gas molecules and membrane materials.[1,7]

In this paper, polymeric, asymmetric and composite membrane was used for water vapor-N_2 mixed gas separation to develop the intrinsic performances of flue gas dehydration system as well as has been researched for natural gas dehydration, drying of compressed air, and organic compound dehydration.[8-10] Interfacial polymerization process on pristine porous substrate was carried out for fabrication of thin film composite (TFC) membrane because the process shapes uniform and rigid micropores in the cross-linked layer,[11] leading to a good candidate of high separation factor and chemical resistance for gas separation membrane.[12,13]

3,5-diaminobenzoic acid (BA) containing both amine and carboxylic acid groups was used as an aqueous monomer and reacted with trimesoyl chloride (TMC). In fact, this aqueous monomer has ever been researched in terms of improvement of membrane properties namely for reverse osmosis. Recently, A. Mehrparvar et al. modified and prepared nanofiltration membrane with a blending method by using 3,5-diaminobenzoic acid and gallic acid as additives. This work researched how the two types of hydrophilic monomers affected the morphology, performance, and antifouling properties of membranes. These membranes performed pure water flux but aimed at humic acid separation.[14] A. L. Ahmad et al. used 3,5-diaminobenzoic acid to fabricate polyamide for reverse osmosis membrane.[15] Even if the effect of 3,5-diaminobenzoic acid content on pore size, flux and rejection was evaluated, the material was added to prepare 3,5-diaminobenzoylpiperazine as a dimer and the factor of diamine ratio with piperazine was investigated. A few years later, results of variation in monomer type including 3,5-diaminobenzoic acid were obtained by N. K. Saha et al. in 2009.[16]

Based on the aforementioned researches, the productive materials were synthesized by 3,5-diaminobenzoic acid and applied for polymeric gas separation membrane. Especially, it is considered that a way to select the unaccustomed material and focus on the effects of preparation conditions, such as concentration of aqueous phase monomer and reaction time, plays an important role in applications of polymeric membrane since the topics of this study specialized in water vapor permeation, which has been rarely interesting for gas separation membrane. The performances of the fabricated membranes for water vapor/N_2 mixed gas by using interfacial polymerization technique were presented in this work. In addition, the various and attentive results by characterization with ATR-FTIR, XPS, FE-SEM and water contact angle were included with elaboration in this paper for providing the knowledge and material for the further application of membrane.

2. Experimental

2.1 Membrane preparation

2.1.1 Materials

Polyethersulfone (PES, Ultrason® E6020P, BASF, Germany) and lithium chloride (LiCl, Sigma-Aldrich) as pore former were used as received. N, N-dimethylformamide (DMF, SAMCHUN chemicals) as a solvent was used to prepare for film type of support layer. 3, 5-diaminobenzoic acid (BA) and trimesoyl chloride (TMC) were purchased from Sigma-Aldrich as monomers for interfacial polymerization. BA is an easily soluble monomer in deionized water and n-hexane (99.9%, Fisher Scientific, NJ) was used as a solvent for TMC. For water vapor/N_2 mixture gas, feed gas was pure nitrogen (99.9%) and vaporized by deionized water (DI) from a Milli-Q ultrapure water purification system (Millipore). All chemical reagents used for this study were used as received.

2.1.2 Polyethersulfone as support layer

The micro-porous, sub-layer **membrane was** prepared by phase inversion technique similar method as discussed elsewhere.[17,18] Lithium chloride was firstly dissolved in N, N-dimethylformamide at 40 °C and polyethersulfone polymer (15 wt. %) powder was dried at 30 °C. The dried PES was dissolved in N, N-dimethylformamide containing LiCl under continuous stirring for 10 hours to get homogeneous solution at 40 °C. The polymer solution was evacuated to remove air bubbles and cast on a glass plate (thickness 90-110 µm) using doctor's blade under controlled conditions of temperature (25-26 °C). The membrane was exposed to the air for 30 sec before precipitation in de-ionized water for non-solvent induced phase inversion. The membrane was removed from the precipitation solution after 30 min and washed thoroughly with de-ionized water to remove the remaining solvent.

2.1.3 Preparation of TFC membranes

To synthesize the cross-linked selective layer by interfacial polymerization, 3,5-diaminobenzoic acid (BA) and trimesoyl chloride (TMC) were used as aqueous and organic phase monomers, respectively, and structures of cross-linked amides and esters were illustrated in Fig. 1. BA was introduced as aqueous phase monomer to fabricate TFC membranes because BA has the hydrophilic group of carboxylic acid compared to m-phenylenediamine (mPD) studied before.[19] TMC monomer, which has high reactivity with the other monomer, is commonly used as organic phase. As shown in Table 1, TFC membranes were prepared for the different concentration of BA as well as the reaction time at same concentration of organic monomer. The pristine PES membranes were dried in advance and immersed in

an aqueous solution of BA for 10 min followed by draining off for 2-5 min to remove excess solution. They were then immersed into 0.2 wt. % of TMC in hexane solution for the various desired contact time as shown in Table 1 followed by draining off excess solution.

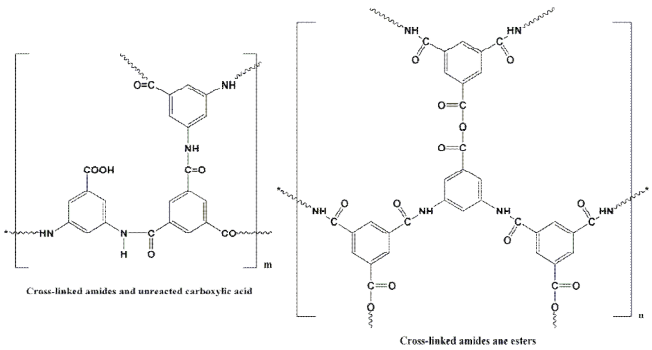

Fig. 1 Chemical structures of (a) cross-linked amides and (b) esters by reaction between 3,5-diaminobenzoic acid and trimesoyl chloride.

Table 1 Series of the conditions for preparation of TFC membranes; the concentration of 3,5-BA and TMC is weight percentages (wt. %).

Series	Membrane	3,5-BA	TMC	Reaction time (min)
1	BA-0.5-3	0.5	0.2	3
	BA-0.5-5	0.5	0.2	5
	BA-0.5-10	0.5	0.2	10
	BA-0.5-15	0.5	0.2	15
2	BA-1-3	1.0	0.2	3
	BA-1-5	1.0	0.2	5
	BA-1-10	1.0	0.2	10
	BA-1-15	1.0	0.2	15
3	BA-2-3	2.0	0.2	3
	BA-2-5	2.0	0.2	5
	BA-2-10	2.0	0.2	10
	BA-2-15	2.0	0.2	15

2.2 Intrinsic properties of TFC membranes

2.2.1 ATR-FTIR

ATR (Attenuated Total Reflectance)-FTIR (Fourier transforms infrared spectroscopy) is an useful and desirable technique for samples, such as the surface of polymer, some adhesives or sponge-like material, which have some difficulties in preparation for analysis at dispersive IR. Verification for the presence of certain functional groups, attributed to interfacial polymerization process on sub-layer surfaces, was conducted by FTIR for surface chemistry of real specimens. Results of FTIR spectrums were obtained by ALPHA-P Spectrometer (Bruker Optic GmbH) with diamond crystal in the range of 600-4000 cm^{-1}.

2.2.2 XPS

XPS (X-ray Photoelectron Spectroscopy) known as ESCA (Electron Spectroscopy for Chemical Analysis) is able to examine the element compositions on surface of thin films. The analysis was conducted by using MultiLab 2000 (Thermo Scientific, USA). 650 micrometre was set in the system for the specific spot size. TFC membranes were surveyed and continuously recorded with the range from 0 to 1100 eV.

2.2.3 FE-SEM

The prepared TFC membranes were characterized by scanning electron microscope (SEM, S-4700, Hitachi). The morphologies and thickness of selective layer were examined in type of cross-section images. Membrane samples were firstly moisturized by distilled water, frozen and fractured in liquid nitrogen. Before scanning, the specific area of samples was covered with a thin layer of gold by using Sputtering apparatus (Balzers Union SCD 040).

2.2.4 BET surface area analysis

The modified membranes were characterized by BET surface area analyzer to verify whether the potential voids exist on the membrane surface or not. BET analysis technique is possible to evaluate the active surface area and pore size distribution. Based on the principle of physical gas adsorption the surface area of thin film composite polysulfone flat sheet membrane was calculated by the Brunauer–Emmett–Teller (BET) method using Micromeritics ASAP 2020 analyzer, and the pore size distribution was calculated by the Barrett–Joyner–Halenda (BJH) method. The adsorption test was conducted under nitrogen gas condition.

2.2.5 TGA analysis

As a method of thermal analysis, substrate and TFC membranes were characterized by using TGA/DSC1 (Mettler-Toledo International Inc., Switzerland). TGA (Thermo-gravimetric analysis) is a proper method to quantitatively examine the polymer materials since the decomposition kinetics is dependent on a type of polymer at a region where it is combusted. All samples were tested under the N_2 atmosphere up to 700 °C with a heating rate of 10 °C/min.

2.2.6 Water contact angle

The surface of pristine substrate as well as all modified membranes was evaluated by contact angle drop shape geometry (DSA100, Germany) using Milli-Q deionized water as the probe liquid at room temperature. To minimize the experimental error, the contact angle was randomly measured at more than 10 different locations for each sample and the average value was reported.

2.3. Performances of TFC membranes for water vapor permeation

Schematic system for water vapor separation from vapor-N_2 mixed gas is illustrated in Fig. 2. Relative humidity of mixed gas flowing through the permeation cell should be steady state by controlling the distilled water flow rate from HPLC pump and the constant proportion of carrier gas to dilution gas flow rate. Demister removed the water droplets in mixed gas. In order to provide the desired vacuum (0.2 bar), which minimizes the pressure drop, a vacuum pump was connected to the permeate stream during the permeation tests. Back pressure regulator was connected to retentate side so as to operate under the pressure at 3 kg_f /cm^2. HMT (Humidity and temperature transmitter, Probe type 344 Vaisala Oyj, Finland) was used to measure the relative humidity of feed and retentate streams. Permeation test was carried out inside the homoeothermic oven at 30 °C as constant temperature. Mixed gas was separated through TFC membrane and nitrogen gas from permeate and retentate streams was measured by bubble flow meter (Gilibrator, USA) after removing the contained water vapor through cold trap bath (CTB-10, JEIO

Tech., Korea). Evaluation of water vapor permeance requires a specialized calculation as shown in an equation below.

$$Q_{vapor} = \frac{Q_{N_2}\gamma_{H_2O}V_m}{M_{W,H_2O}} \quad (1)$$

Q_{N2} (cm^3/s) from each of the retentate and permeate stream is measured by bubble flow meter after the iced cold trap. γ_{H2O} is the absolute humidity (g/m^3) and V_m is the volume of 1 mol penetrant at standard temperature and pressure (22.4 ℓ/mol). $M_{w,H2O}$ is the molecular weight of water (18 g/mol) and Q_{vapor} (cm^3(STP)/s) is finally determined.

For thin film composite membranes, permeance (P_i/ℓ) is used to evaluate their performances because the thickness of thin selective layer is unable to accurately be measured. Permeance of component *i* in mixture gas is determined by equation as follows.

$$\frac{P_i}{l} = \frac{Q_i}{A \cdot \Delta p_i} = \frac{N_i}{(p_{i,feed} - p_{i,permeate})} \quad (2)$$

Permeance (P_i/ℓ) is commonly obtained in gas permeation unit (GPU, 1 GPU=10^{-6} cm^3(STP)/(cm^2·sec·cmHg)). N_i is the flux (L/m^2h) at permeate stream through the film by dividing Q_i with effective area of film membrane A (cm^2). Δp_i of component *i* is the partial pressure difference (cmHg) between feed and permeate side. The partial pressures, $p_{i,feed}$ and $p_{i,permeate}$, on feed and permeate sides is calculated by multiplying total pressure by mole fraction under same temperature and pressure. The separation factor ($\alpha_{i/j}$) of the membrane for gas *i* is the ratio of their gas permeance and calculated by

$$\alpha_{i/j} = \frac{P_i/l}{P_j/l} \quad (3)$$

3. Results and discussion

3.1. Intrinsic properties of TFC membranes

Four types of characterization methods were used to verify the improvement of TFC membrane in terms of physicochemical properties for the different concentration of BA and reaction time for interfacial polymerization. ATR-FTIR and XPS (ESCA) were employed to confirm the existence of functional groups and the chemical compositions on the modified surface of TFC membranes.

3.1.1 ATR-FTIR

Figure 3 shows IR spectra of PES substrate and TFC membranes. Except for PES, IR peaks at 1540 cm^{-1} and 1692 cm^{-1} of all TFC membranes displayed in Fig. 3 were obtained due to stretch vibrated N-H and C=O of amide, respectively. Bending vibration of N-H amide appeared at 1630 cm^{-1}. Spectra at 770 cm^{-1} were specially detected due to the vibration of C-Cl stretch, which consists of the unreacted and remaining carbonyl chloride in three-functional trimesoyl chloride. Additional peaks at 925, 1300 and 1721 cm^{-1} remarkably detected at BA-2-15 membrane were ascribed to the highest concentration of BA and reaction time with TMC. Spectrum at 925 cm^{-1} and 1721 cm^{-1} corresponds to vibrations of O-H bend and C=O stretch in carboxylic acid, respectively. They can prove that the hydrolysis of –COCl occurred during the polymerization. Peak at 1300 cm^{-1} is considered close to the carbon stretch (C-O) connected to –OH in carboxylic acid.

To investigate some changes attributed to polymerization conditions such as monomer concentration and reaction time, intensity of absorption at the specific range of wavenumber was analyzed. Fig. 4 was illustrated to compare the IR absorbance of TFC membranes synthesized by different monomer concentration. Even though BA-1-5 membrane showed the week intensity of N-H amide, all amide was confirmed on three of the TFC membranes. As expected for the effect of increased monomer concentration, BA-2-5 membrane spectra showed that C=O and O-H bends of hydrophilic carboxylic acid group were also remarkably detected at 1721 and 2600 cm^{-1}, respectively.[15]

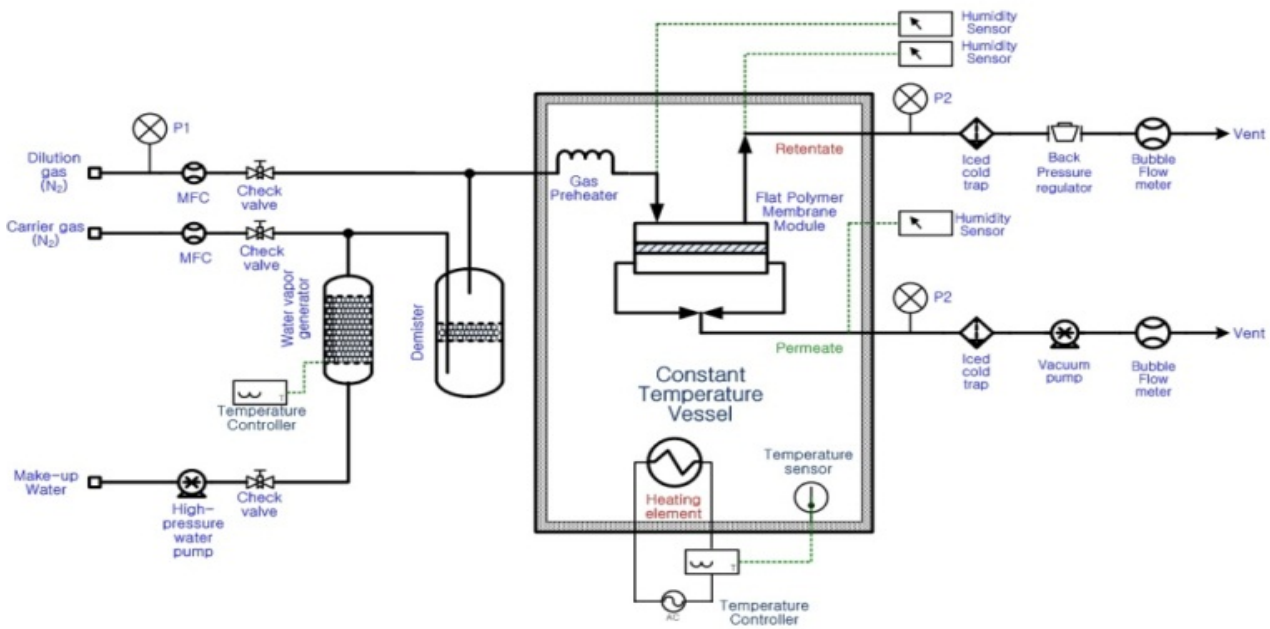

Fig. 2 Schematic system for water vapor permeation through TFC membranes.

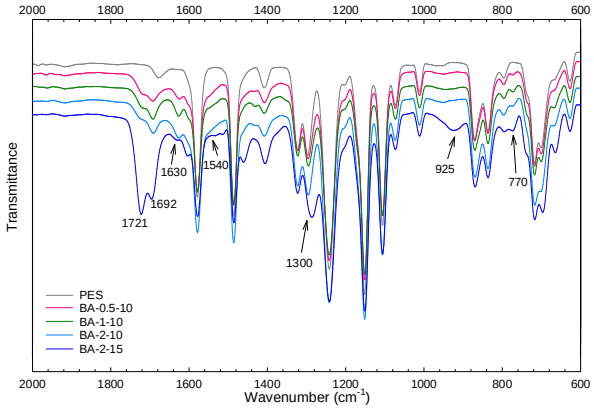

Fig. 3 ATR-FTIR spectra of PES substrate and TFC membranes

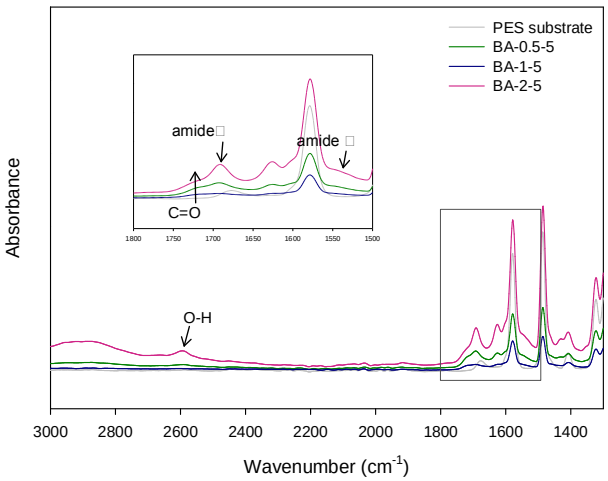

Fig. 4 IR absorbance of membranes for different concentration of BA at 5 min reaction time

Figure 5 was depicted to show the effect of different reaction time at 2.0 wt. % of BA. In all TFC membranes prepared by various contact time, stretch vibrations of amides at 1540 cm^{-1} and 1692 cm^{-1} were detected. The peak at 1630 cm^{-1} is due to N-H bend vibration. In this spectra for different reaction time at 2.0 wt. % of BA, absorptions at 1300 cm^{-1} and 1721 cm^{-1} were detected due to C-O and C=O, respectively, by cross-linked ester appeared as expected.

The magnified figure was inserted to see the distinction of intensity at 760-780 cm^{-1} by C-Cl stretch vibration. Apart from PES substrate, all TFC membranes had C-Cl group and its difference in absorbance due to the unreacted TMC. The peak for C-Cl stretch gradually existed as the reaction time increases, and then finally disappeared at BA-2-15 membrane. The decrease of the peak, while reaction time increases, means that the unreacted carbonyl chloride of TMC exactly reacted with BA monomer. The reaction can occur with amine and/or carboxylic acid in BA. If it reacts with amine, polyamide peak would improve. However, if it reacts with carboxylic acid, the ester may be formed in the selective layer. As a result shown in Fig. 5, distinct additional peak at 1721 cm^{-1} can be considered C=O of ester because the absorbance was higher than the lower N-H amide peak at BA-2-15 membrane.

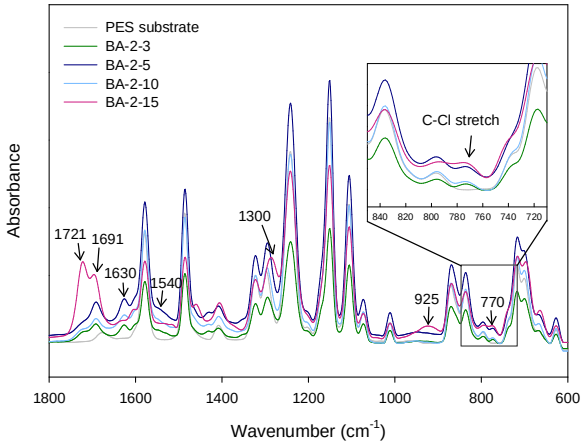

Fig. 5 IR absorbance of membranes for different reaction time with 2.0 wt. % BA

3.1.2 Thickness of selective layers

As the thickness of selective layer on polyamide nanofiltration membranes had been determined by measurements of peak intensities, the quantitative thickness of thin films was also determined through the results of IR spectra in this study following equations reported by Oldani and Schock.[16,20,21]

$$d_p = \frac{\lambda / n_1}{2\pi\left\{\sin^2\theta - \left(\frac{n_2}{n_1}\right)^2\right\}^{1/2}} \quad (4)$$

$$l = d_p \times I_{peak} \quad (5)$$

For the certain region of wavelength 2.5 to 16 ㎛, the radiation penetration depth ranges from 0.48-3.1 ㎛. The penetration depth for IR, d_p, was constantly determined. IR incident angle (θ) was 45° and, assuming the refractive index of the polymer (n_2) to be 1.5 (mostly 1.5-1.6 for polymers), the depth for radiation penetration is dependent upon the refractive index of IR spectrometer crystal (n_1). For diamond crystal used in this characterization, the refractive index is 2.42.

The thickness of selective layer for each of TFC membrane was calculated by multiplying d_p corresponding to the amide Ⅰ frequency (1625 cm^{-1}) by the absorbance intensity. The calculated thickness of selective layer was shown in Table 2 and drawn in Fig. 6 as a function of reaction time. The higher concentration of BA increased thickness of selective layer at reaction time from 3 min to 10 min. At 15 min of reaction time, the thickness decreased at BA-1-15 and then increased to 43 nm at BA-2-15.

The longer reaction time of TMC with BA also increased the thickness. The lowest concentration, 0.5 wt. % of BA, showed the linear correlation with reaction time until 10 min. At 1.0 wt. % and 2.0 wt. % of BA, the highest thickness was obtained as 48.47 nm and 77.65 nm at 10 min and 5 min reaction time, respectively. The growth of thickness of selective layer on TFC membranes is dependent upon degree of cross-linking polyamide when the another diamine of BA react with the unreacted terminal acid chloride of TMC.[20,22] Therefore, the results of Table 2 obtained by the intensity peak at amide would help to support the change and different at performances such as flux and permeance of

water vapor separation.

Table 2 Thickness of selective layer on TFC membranes by using the absorption peak of FT-IR

Membrane	Intensity (absorbance)	Thickness (nm)
BA-0.5-3	0.0094	11.19
BA-0.5-5	0.0261	31.04
BA-0.5-10	0.0385	45.77
BA-0.5-15	0.0308	36.55
BA-1-3	0.0106	12.59
BA-1-5	0.0280	33.26
BA-1-10	0.0408	48.47
BA-1-15	0.0188	22.33
BA-2-3	0.0347	41.20
BA-2-5	0.0654	77.65
BA-2-10	0.0533	63.32
BA-2-15	0.0336	39.88

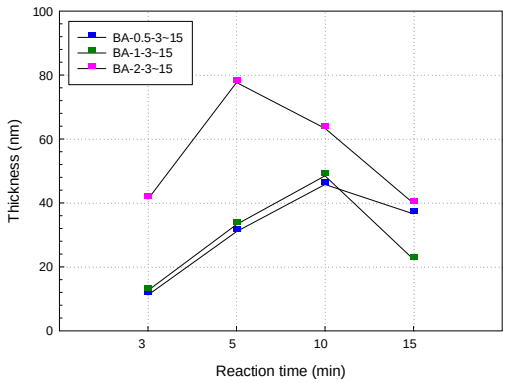

Fig. 6 Calculated thickness of selective layers based on the results of IR absorbance

3.1.3 XPS analysis

Chemical components of TFC membranes were analyzed by XPS (X-ray Photoelectron Spectroscopy) and summarized in Table 3 for different concentration monomer and reaction time. As mole ratio of atomic element can generally be contrasted with theoretical values by repeating unit,[23] we expected two types of cross-linked structures shown in Fig. 1 and their theoretical values of N/O, N/C, and O/C at cross-linked amide were 0.5, 0.133, and 0.266. The O/C molar ratio of cross-linked ester is 0.313, which is higher than cross-linked amide, whereas N/O and N/C molar ratio are lower as 0.4 and 0.125 than the amide, respectively.

PES substrate was only composed of carbon and oxygen. For TFC membranes synthesized by BA and TMC, different percentages of oxygen as well as nitrogen were detected. For the effect of BA concentration at 10 min of constant reaction time, carbon percentage increased whereas oxygen decreased. In particular, nitrogen and oxygen decreased at BA-1-10 membrane but increased later at BA-2-10 membrane. Compared to nitrogen ratio, such as N/O and N/C, oxygen ratio at O/C constantly decreased with the increment of BA concentration.

It is suggested that proper concentration of BA is able to synthesize the desired, cross-linked and selective layer. For the effect of reaction time at 2.0 wt. % of BA, nitrogen ratios were all lower than the theoretical values of amide and ester. However, O/C at BA-2-3 membrane was between 0.266 and 0.313. It is considered that cross-linked amide and ester coexist on TFC membrane, including unreacted carboxylic acid. Oxygen percentage also constantly decreased as the reaction time increased. Nitrogen percentage and ratio, compared to other components, increased at BA-2-5 membrane and then, decreased at higher concentration.

To examine the spectra for binding energy of TFC membranes, deconvolutions of C1s and O1s by curve fitting are shown in Fig. 7 and 8. This analysis by data fitting was based on the data supplied in reference.[24] Fig. 7 depicts the distinct peaks at high resolution C1s of TFC membranes for different concentration of BA at 10 min. BA-0.5-10 membrane had two major peaks at 285 and 289 eV. By curve fitting of the spectra, additional peak at 288 eV was detected. The major peaks are ascribed to C-C/C-H and O=C-O. The minor peak of 288 eV is C=O. All peaks were also obtained in BA-1-10 membrane whereas BA-2-10 membrane only exhibited one peak at 285 eV by curve fitting. As BA concentration increases in Fig. 7, the number of peaks reduced and they were almost about carbonyl groups of carboxylic acid and ester. The change of spectra probably means that increase of BA concentration is able to diffuse onto the interface for polymerization, leading to disappearance of peaks at 288 eV because of the actively consumed C=O in carboxylic acid. According to Table 3, however, since oxygen percentages of BA-2-10 membrane were obtained, O1s analysis for high resolution was conducted to verify the existence of oxygen related to esters or carboxylic acid.

Table 3 Atom percentages on substrate and modified surfaces of TFC membranes by XPS spectrum measurement

Membrane	C	N	O	N/O	N/C	O/C
PES [a]	82.35	-	17.65	-	-	0.214
BA-0.5-10	72.91	2.26	24.83	0.091	0.031	0.341
BA-1-10	75	1.58	23.42	0.067	0.021	0.312
BA-2-3	76.99	1.58	21.44	0.071	0.020	0.278
BA-2-5	79.16	2.78	18.06	0.154	0.035	0.228
BA-2-10	80.15	2.21	17.64	0.125	0.027	0.220
BA-2-15	88.22	-	11.78	-	-	0.134

[a] reference [25]. This PES substrate was provided by this study as well.

Figure 8 is a result of O1s deconvolution by curve fitting for TFC membranes. Fig. 8 illustrates the change of peaks at some specific binding energy for different reaction time at 2.0 wt. % of BA. BA-2-3 membrane includes 533.5, 532.7, 532.2 eV, BA-2-5 membrane 532.7, 532.2 eV, BA-2-10 membrane 532.7, 532.2 eV, BA-2-15 membrane 533.5, 532.2 eV. The lowest intensity at 533.5 eV of BA-2-3 membrane describes the minor peak for –O*-(C=O)-. The binding energy at 532.7 eV of BA-2-3 membrane might be obtained due to –(C=O*)-O-(C=O*)- and C-

O-C, which is a part of cross-linked ester groups connected to aromatic rings. TFC membranes polymerized at 2.0 wt. % except for BA-2-15 membrane commonly have a peak at 532.7 eV. This intensity is attributed to the reaction between carboxylic acids to form esters and gradually increased with reaction time increased until 10 min. The intensity at 532.2 eV was detected due to C=O of carboxylic acid in BA-2-3 and BA-2-5 membranes. A peak at 532.2 eV of BA-2-10 and BA-2-15 membranes also exactly notified ester, O-(C=O*) containing carbonyl group. For long contact time 15 min, 533.5 eV suddenly appeared and the intensity at 532.2 eV more increased than 10 min.

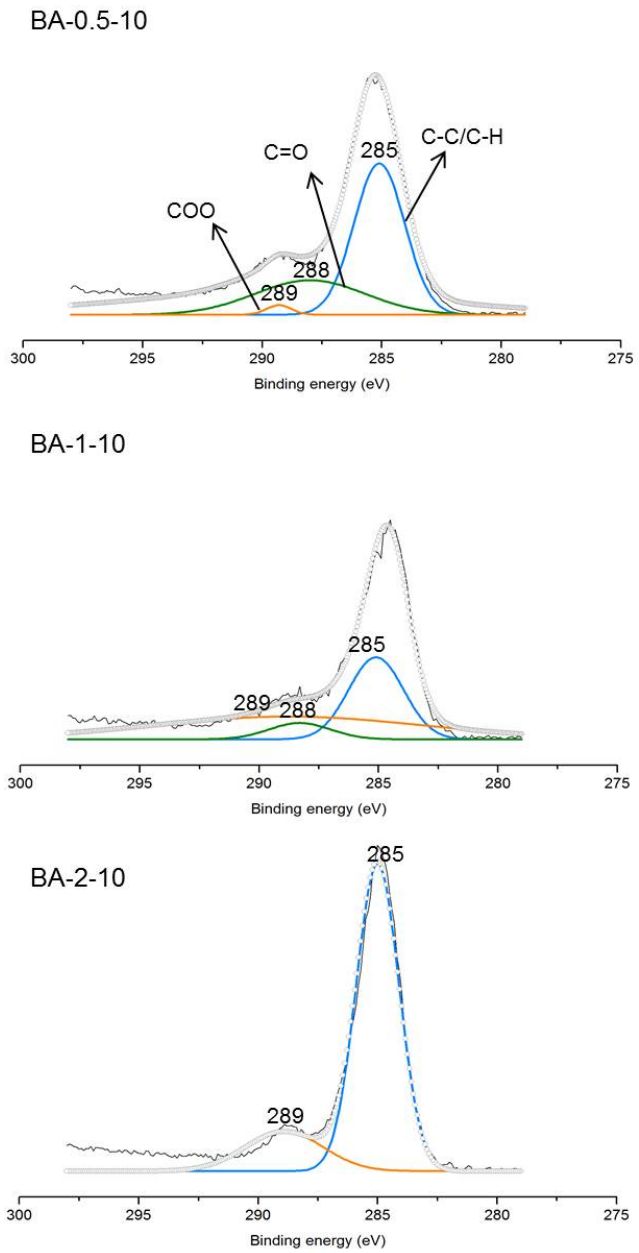

Fig. 7 High resolution C1s of XPS spectra as BA concentration increases at 10 min of contact time

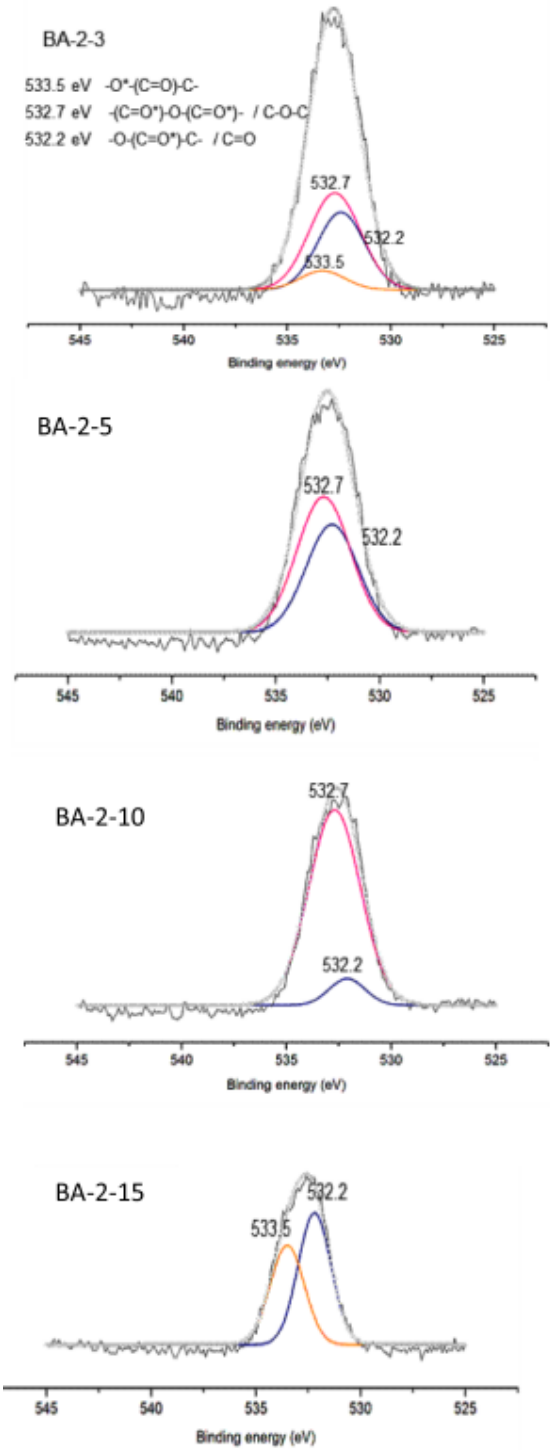

Fig. 8 High resolution O1s of XPS spectra as contact time increases at 2.0 wt. % of BA

3.1.4 FE-SEM analysis

By observation using FE-SEM, cross-sectional and top-view images of TFC membranes were shown in Fig. 9 and Fig. 10 respectively. Fig. 9-(a) is representatively inserted to show how the pores in PES substrate were formed by phase inversion. All TFC membranes fabricated by PES solution dissolved in non-solvent DMF were prepared as shown in Fig. 9-(a). In addition, the other enlarged images of cross section in Fig. 9 show that PA

selective layer was synthesized, making defective surface more compact with transparent or blurred area. Fig. 9-(b) to (d) depicts the modified surfaces for different BA concentration. As shown in Table 3 above, BA-2-5 membrane seems to have the thickest selective layer. As shown in Fig. 9-(d) to (f) obtained at same magnification to evaluate the effect of different reaction time, some differences were observed. Fig. 9-(d) captured with BA-2-5 membrane seems to be denser as well as thicker than Fig. 9-(e) and (f).

As shown in Fig. 10, the upper-side images of TFC membranes were obtained to verify how the selective layer was formed on substrates. In Fig. 10-(a), it was found that the selective layer was synthesized at intervals on BA-1-3 membrane. For the longer reaction time at BA-1-10 membrane, it was observed that selective layer was more densely synthesized, almost showing smooth surface. In comparison with Fig. 10-(a) and (b), surfaces BA-2-3 and BA-2-10 membranes seem to become denser. Some particles detected by SEM observation are considered undesired products of self-polymerization reaction due to the highest concentration of 3,5-BA. Furthermore, as contrasted with the results of calculated thickness in Table 3, it was confirmed why the thickness of selective layer increased for the reaction time and concentration of monomer as expected.

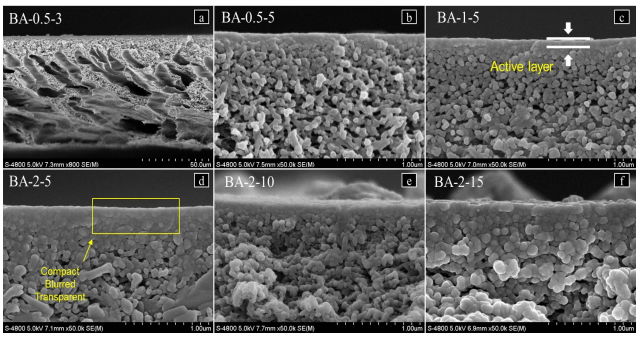

Fig. 9 Cross-sectional images of TFC membranes prepared by 3,5-diaminobenzoic acid

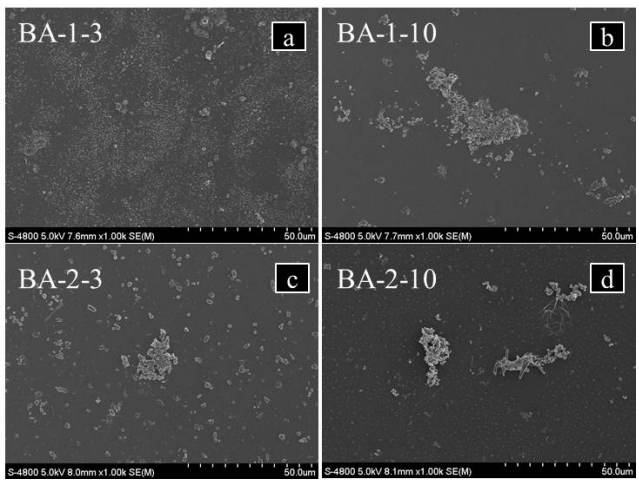

Fig. 10 Top-view images of TFC membranes by 3,5-diaminobenzoic acid.

3.1.5 BET surface area analysis

The surface area of thin film composite polysulfone flat sheet membrane (BA-2-15) was calculated by the Brunauer– Emmett–Teller (BET) method using Micromeritics ASAP 2020 analyzer, and the pore size distribution was calculated by the Barrett–Joyner–Halenda (BJH) method. The porous texture of the membrane BA-2-15 was determined using nitrogen sorption measurements at 77 K with prior activation at 100 °C for 1 h. The nitrogen sorption isotherm of membrane BA-2-15 is shown in Fig. S1 exhibit Type IV behaviour (as per the IUPAC classification) with a hysteresis loop, associated with the filling and emptying of the mesopores by capillary condensation.[26] The BJH pore size distribution is shown in Fig. S2 with desorption data is also showed its mesoporous nature with average pore size of 19.32 nm.

3.1.6 TGA analysis

PES substrate and TFC membranes by 3,5-diaminobenzoic acid were characterized by TGA because water vapour/N_2 mixed gas separation occurs through membranes at an elevated temperature. The results were obtained in view of weight loss and its rate with the increased temperature in Fig. 11. The pristine PES membrane in Fig. 11-(a) started to lose in weight at 53.02 °C, BA-1-15 membrane at 51.28 °C in Fig. 12-(b) and BA-2-15 membrane at 54.27 °C in Fig. 12-(c), respectively. To compare the results of TG analysis for membranes, the rate of weight loss per minute was also evaluated and shown below the typical graphs. All membranes showed that the second loss of weight was found around 200 °C as well as the drastic loss of weight was detected over 450 °C. In particular, BA-1-15 and BA-2-15 membranes showed the third loss of weight at 304.37 °C and 396.36 °C, respectively. Therefore, it is concluded that TFC membranes are able to remain stable (until approximately 300 °C) and show the reliable performances under the elevated temperature.

3.1.7 Water contact angle

Water contact angles of modified surface of TFC membranes were measured and depicted in Fig. 12. The results of BA-0.5-3~15 membranes were colored blue and Fig. 12 shows that their contact angles gradually decreased for prolonged reaction time. The lowest contact angle was 85.3±2°. Contact angles of BA-1-3~15 membranes were unexpectedly different for the increment of reaction time. Especially the angles remarkably increased until 10 min, and then decreased as 88.1±1° at 15 min. Contact angles of BA-2-3~15 membranes were also different for reaction time. In particular, water contact angle of BA-2-5 membrane was the lowest as 86.1±1° and then that of the other two membranes increased for longer contact time. These measured contact angles can be described with carboxylic acid contained in BA aqueous monomer as well as hydrolyzed from carbonyl chloride. Contact angles which do not follow the expected and linear relationship to reaction time or BA concentration are ascribed to the newly cross-linked ester because functional groups like amides and esters are known as more hydrophobic, leading to low solubility of water vapor.[27]

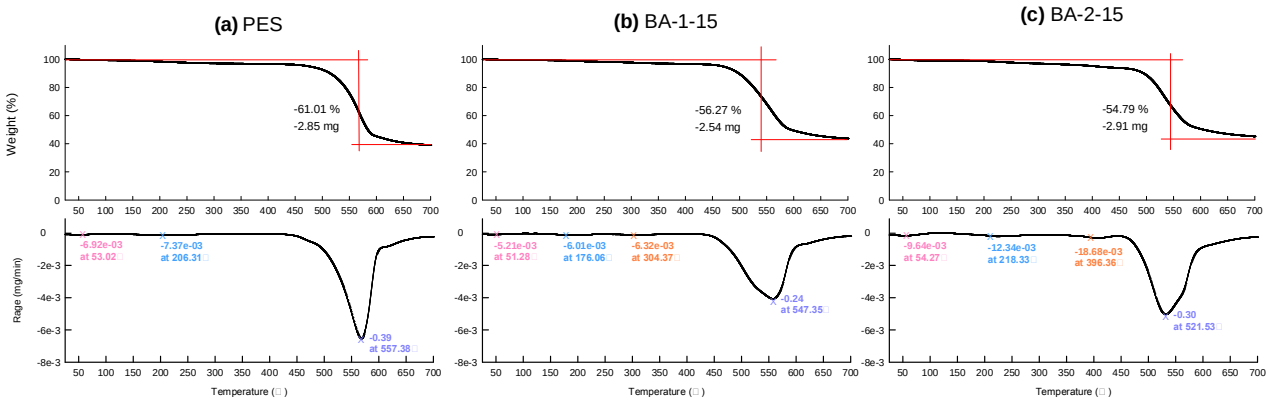

Fig. 11 TGA curves of (a) PES, (b) BA-1-15 and (c) BA-2-15 membranes

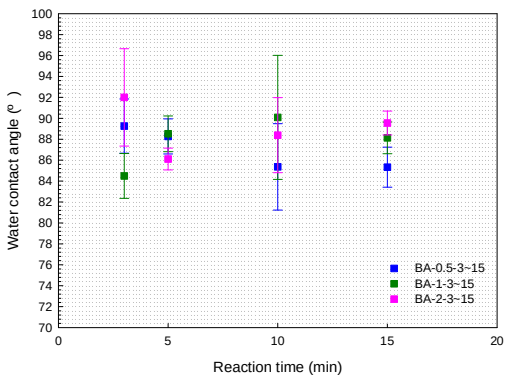

Fig. 12 Measured water contact angle on thin layer of TFC membrane surface

3.2 Water vapor permeation by TFC membranes

3.2.1 Effect of concentration on water vapor permeation

Results of performances for different monomer concentration at constant reaction time are compiled and displayed in Fig. 13. When the results are separated for same reaction time, the effect of BA concentration on membrane performances can be visually observed. As monomer concentration increased, separation factor became improved, whereas permeance of water vapor did not exhibit a routine correlation. In Fig. 13-(a) for 3 min reaction time, when permeance increased and decreased, separation factor also simultaneously became increased and decreased. Water vapour permeance and separation factor of BA-1-3 membrane 2063 GPU and 12, respectively. The increased performances, compared to BA-0.5-3 membrane, are due to the increased concentration of BA. As shown in Fig. S3, intensity (COOH) of BA-1-3 was 0.0160 higher than BA-0.5-3 membrane. Therefore, it was confirmed that 1.0 wt. % of BA have more carboxylic acid in monomer than 0.5 wt. % of BA, which make the membrane surface hydrophilic, planar and compact.[15,16] The higher separation factor of 1.0 wt. % than 0.5 wt. % is attributed that higher concentration of BA faster diffuses up to the interface and then, reacts with organic monomer, which vertically exalts the degree of crosslinking amide on membrane surface.[28] Contact angle of BA-1-3 was 84.5±2° and lower than that of BA-0.5-3 as well. BA-2-3 membrane was firstly considered a factor to incur the growth of selective layer thickness, which incurs the decrease of performance. Meanwhile, contact angle of BA-2-3 membrane was over 90 °, which means that the coated surface becomes less hydrophilic. In spite of the detected carboxylic acid in BA-2-3 membrane, spectra of IR showed that BA-2-3 membrane also includes higher peak of amides (Fig. S3), which are considered as hydrophobic compounds.[27] Therefore, it is suggested that 2.0 wt. % of BA be possibly able to polymerize itself when surface of PES membrane are exposed to the aqueous monomer for immersion. In addition, the higher concentration more affects the degree of cross linking, horizontally and tightly blocks the pores on PES surface, and finally reduces the membrane performances.[13,22] That leads to densification of selective layer,[16] by consuming the carboxylic acid in monomer and forming esters. According to the results of Table 2 and Fig. 6, despite the increased thickness of selective layer at higher concentration, it is concluded that membrane performances are readily more dependent on hydrophilicity and inclination of packed structures and morphologies than on thickness of selective layer because changes in flux as well as permeance of water vapor were equally same as a function of BA concentration (Fig. S4).

Apart from results in Fig. 13-(a), TFC membranes prepared by different concentration of BA showed that separation factor almost had similar trend at constant reaction time. It is observed that separation factor was gradually improved as BA concentration increases. Results of Fig. 13-(b) and (d) indicate that separation factor increased whereas permeance decreased for the increase of monomer concentration. It is verified that, when the reaction occurs for more than 5 min at the interface with BA monomer, “trade-off” phenomena can be generally observed in membrane separation.[13,29] Contact angles of the membranes gradually increased up to 89.5±1° with BA concentration increased in accordance with water vapor permeance at 15 min of reaction time in Fig. 13-(d). On the other hand, Fig. 13-(c) shows that water vapor permeance was a little improved at 1.0 wt. % (BA-1-10 membrane), but the value was almost constant with 0.5 wt. %. Furthermore, each contact angle of TFC membranes at 10 min of reaction time was included in one another’s standard deviation, which means that the angles are not largely different. Through the results of atomic contents on TFC membranes of Fig. 13-(c), the increase in carbon implies that the effect of BA concentration influences the polymerized selective layer. Permeance a little increased when N and O decreased at BA-1-10 membrane, whereas the permeance was lower at BA-2-10

membrane when N increased. This result indicates that increase in content N negatively affects water vapor permeance.

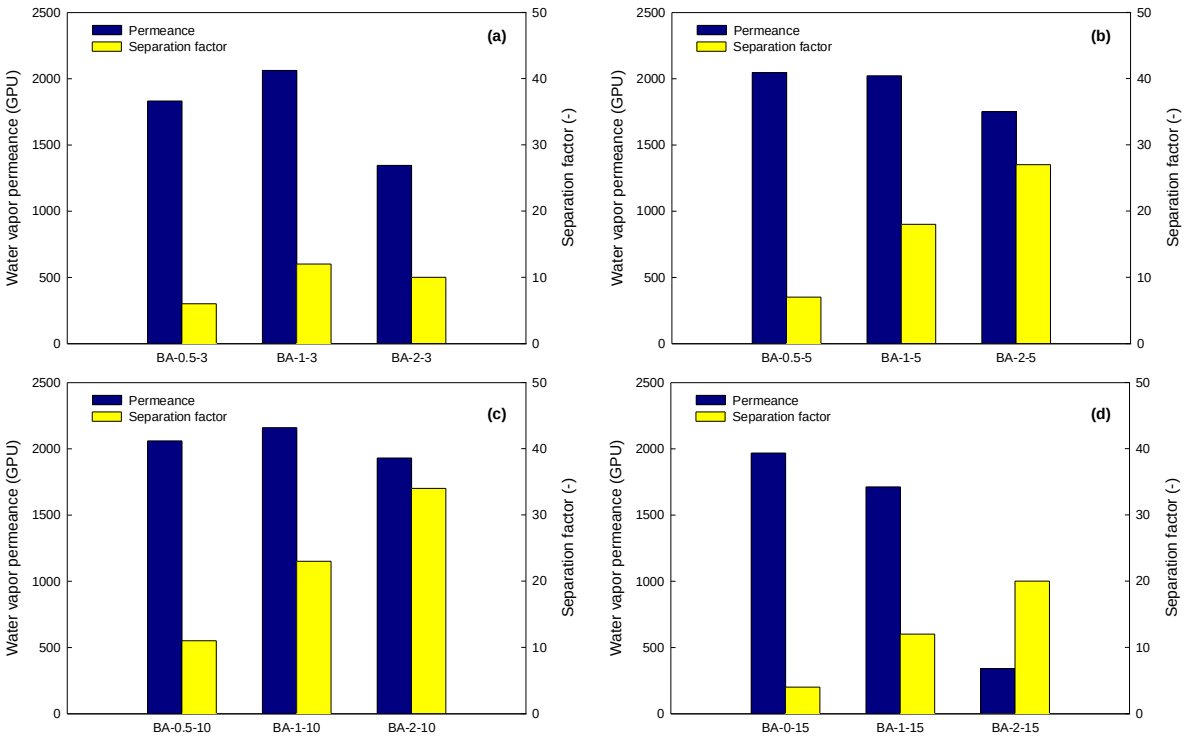

Fig. 13 Correlation between performances and BA concentration at constant reaction time; (a) 3 min, (b) 5 min, (c) 10 min and (d) 15 min.

As shown in Fig. 13 for the factor of BA concentration, an increase of BA concentration has an ability to improve both permeance and separation factor until limited reaction time (<15 min). However, 2.0 wt. % of BA only improved separation factor since it is easier enough to make the selective layer more compact than 1.0 wt. % of BA by forming hydrophobic cross-linked esters. In order to overcome demerits in performances of membrane separation, such as "trade-off" phenomena, reaction with functional organic solvent should be conducted as short as optimized to fabricate thin film layer.

3.2.2 Effect of reaction time on water vapor permeation

Figure 14 is constructed to illustrate the change of performances as a function of reaction time at the each constant concentration of aqueous monomer. Fig. 14-(a) signifies the similar changes in permeance and separation factor of water vapor. As the reaction time increased up to 10 min at 0.5 wt. % of BA, permeance and separation factor increased. However, performances decreased at 15 min of reaction time with TMC. The trend of water vapor permeance until 10 min is ascribed to the hydrolysis of unreacted -COCl, which brings the improvement in hydrophilicity on active layer of TFC membrane, compared to the hydrophobic pristine substrates. Besides, intensity (COOH) of TFC membranes increased as reaction time increased (Fig. S5). As shown in Fig. 12, contact angles also steadily decreased with long reaction time and became constant as 85.3±2°. In addition, increase of separation factor, in spite of the increased permeance, is attributed to the synthesized polyamide which inhibits nitrogen from permeating through the membrane. For the further 15 min of reaction time, it is supposed that comparatively high permeance be obtained due to the hydrolysis of -COCl for long reaction time, but permeance slightly decreased. IR of TFC membranes for different reaction time at 0.5 wt. % of BA is shown in Fig. S5. C=O of carboxylic acid as the pendant was detected up to 0.034 (intensity of COOH) due to the unreacted and hydrolyzed -COCl of TMC as the reaction time increased. On the other hand, separation factor was the lowest at 15 min since nitrogen permeance basically increases due to the coalescence of adjacent pores that becomes defective.[15] In terms of results of thickness in Fig. 6, the decrease at BA-0.5-15 means that absorbance of the amide decreased and it led to increase on porosity of selective layer.[16]

Performances in Fig. 14-(b) were obtained at 1.0 wt. % of BA. Contact angle was lowest as $84.5 \pm 2°$ at 3 min in Fig. 12, showing the high permeance of water vapor. It is considered that decrease of permeance at 15 min is ascribed to the reaction between unreacted -COOH in BA and hydrolyzed -COCl in TMC, resulting in formation of ester which is also more hydrophobic than amide.[27] Before 15 min of reaction time, BA-1-3~10 membranes have esters in active layer as well. However, the high permeance obtained through the membranes is caused by the existence of the unconsumed carboxylic acid. It is suggested that the excessive reaction time such as 15 min hydrolyze COCl to COOH and lead to condensation reaction itself for esters, which simultaneously increases separation factor. In addition, N_2 permeance dramatically increased at 15 min due to the coalescence of adjacent pores by cross-linked polyester,[15,16] and finally separation factor decreased in Fig. 14-(b) with permeance of water vapor decreased.

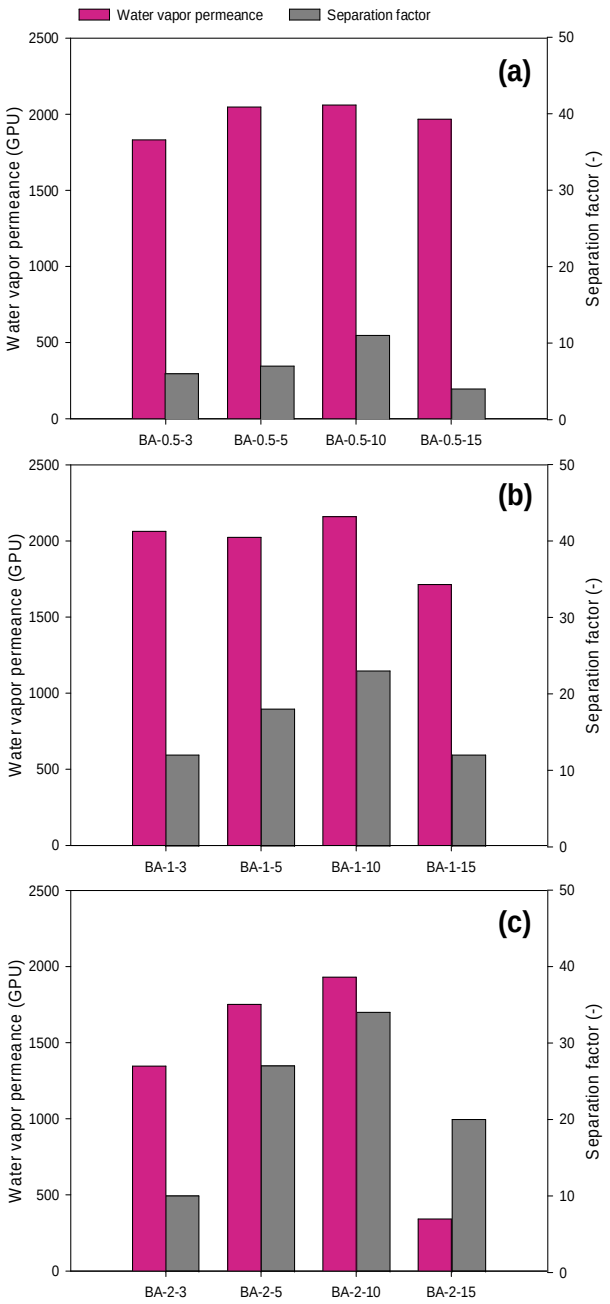

Fig. 14 Correlation between performances and reaction time at constant concentration of BA; (a) 0.5 wt. %, (b) 1.0 wt. % and (c) 2.0 wt. %.

The performances at 2.0 wt. % of BA also illustrated similarity in Fig. 14-(c) for different reaction time. They both increased until 10 min of reaction time and then, decreased at 15 min. Following the IR results in Fig. 5, the reason for increase of water vapor permeance until 10 min is considered attributable to the hydrolyzed COOH from COCl in TMC in spite of the decrease in N_2 permeance, which means pores on selective layer are blocked and nitrogen carrier gas is difficult to accompany the water vapor to permeate side.[11] As reaction time increases in Fig. 12, contact angles decreased as 88.4±3° at 10 min and water vapor permeance of BA-2-10 membrane was 1931 GPU. At 15 min of reaction time, it is supposed that carbonyl chloride is excessively hydrolyzed due to the long exposure time of TMC and the hydrolyzed carboxylic acid forms cross-linked ester on selective layer, and water vapor permeance drastically decreased. N_2 permeane of BA-2-15 membrane was 17 GPU, which was the lowest of all TFC membranes. As illustrated in Fig. 5, OH bending vibration of carboxylic acid was detected at 925 cm^{-1} in BA-2-15 membrane, but this hydrophilic group was not enough to improve the water vapor permeance at higher reaction time than 10 min because much more carboxylic acid reacted with each other. In addition, more cross-linked ester was detected as the remarkable peak at 1721 cm^{-1} (Fig. 5) and the contact angle increased to 89.5±1 ° again at 15 min as well. Ester is possibly considered a minor factor to improve the hydrophilicity on TFC membranes. For the effect of reaction time with TMC, as reaction time increased, separation factor constantly increased until 10 min at each same concentration of BA while permeance was non-linear and different. In particular, all permeance of same concentration certainly decreased at 15 min.

Conclusions

Effects of 3,5-BA concentration and contact time with TMC on membrane performances were mainly evaluated in this paper. Possibility that TFC membrane has esters as well as amides due to carboxylic acid by interfacial polymerization was firstly suggested based on chemical structures of synthesized polymer as products in Fig. 1. The existence of C=O ascribed to esters and amides were verified through the spectra of ATR-FTIR. Furthermore, the data of IR were distinguished by using XPS (ESCA). As contrasted with the results of calculated thickness, vapor flux and permeance (Fig. S4), it is considered that the effect of selective layer growth on water vapor permeance was little and could be negligible. Selective layers of TFC membranes were ascertained in FE-SEM and their hydrophilicity was analyzed by water contact angle. As a result, the highest value of water vapor permeance was 2160 GPU and the highest separation factor in water vapor/N_2 mixed gas was 34 at BA-1-10 membrane and BA-2-10 membrane, respectively. Especially, BA-1-10 membrane has both higher permeance and separation factor as 2160 GPU and 23. It is suggested that higher concentration of BA containing carboxylic acid is possible to diffuse faster, react more actively and form hydrophobic esters. For the long reaction time, the unreacted COCl of TMC is hydrolyzed to COOH and increases the hydrophilicity for better sorption of water vapor. However, the hydrophobic esters can be generated on selective layer due to the longer reaction time over 10 min. Therefore, contact time of TMC should be almost same as immersion time of BA on substrates (10 min) and 2.0 wt. % of BA was proper to obtain the high performances of TFC membranes fabricated by using 3,5-BA and TMC.

Acknowledgements

This work was conducted under the framework of Research and Development Program of the Korea Institute of Energy Research (KIER) (B5-2457).

Notes and references

[a]Korea Institute of Energy Research, 71-2 Jang-dong, Yuseong-gu, Daejeon, Korea.

[b]Department of Chemical and Biomolecular Engineering, Yonsei University, Korea
[†]Equal contribution of both authors.
*Corresponding author: Tel.: +82-42-860-3647; Fax: +82-42-860-3134
Email address: hklee@kier.re.kr (Hyung Keun Lee)
Electronic Supplementary Information (ESI) available: [details of any supplementary information available should be included here]. See DOI: 10.1039/b000000x/

1 S. J. Kim and Y. M. Lee, *Progress Polymer Science*, 2014, http://dx.doi.org/10.1016/j.progpolymsci.2014.10.005.
2 B. Bolto, M. Hoang and Z. Xie, *Water Research*, 2012, **46**, 259-266.
3 A. Ito, Y. Feng and H. Sasaki, *Journal of Membrane Science*, 1997, **133**, 95-102.
4 F. Ahmad, K. K. Lau, S. S. M. Lock, S. Rafiq and A. U. Khan, *Journal of Industrial and Engineering Chemistry*, 2015, **21**, 1246-1257.
5 A. Basile and F. Gallucci, Membranes for membrane reactors: preparation, optimization and selection, 1st Ed., John Wiley and Sons, 2011.
6 K. H. Kim, P. G. Ingole, S. H. Yun, W. K. Choi, J. H. Kim and H. K. Lee, *Journal of Chemical Technology and Biotechnology*, 2014, DOI: 10.1002/jctb.4421.
7 J. R. Du, L. Liu, A. Chakma and X. Feng, *Chemical Engineering Science*, 2010, **65**, 4672-4681.
8 H. Sijbesma, K. Nymeijer, R. van Marwijk, R. Heijboer, J. Potreck and M. Wessling, *Journal of Membrane Science*, 2008, **313**, 263-276.
9 S.R. Reijerkerk, R. Jordana, K. Nijmeijer and M. Wessling, *International Journal of Greenhouse Gas Control*, 2011, **5**, 26-36.
10 H. Lin, S.M. Thompson, A. Serbanescu-Martin, J.G. Wijmans, K.D. Amo, K.A. Lokhandwala and T.C. Merkel, *Journal of Membrane Science*, 2012, **413**, 70-81.
11 C.W. Tsai, C. Tasi, R.C. Ruaan, C.C. Hu and K.R. Lee, *ACS Applied Materials & Interfaces*, 2013, **5**, 5563-5568.
12 H.M. Chen, W.S. Hung, C.H. Lo, S.H. Huang, M.L Cheng, G. Liu, K.R. Lee, J.Y. Lai, Y.M. Sun, C.C. Hu, R. Suzuki, T. Ohdaira, N. Oshima and Y.C. Jean, *Macromolecules*, 2007, **40**, 7542-7557.
13 F. Yuan, Z. Wang, S. Li, J. Wang and S. Wang, *Journal of Membrane Science*, 2012, **421-422**, 327-341.
14 A. Mehrparvar, A. Rahimpour and M. Jahanshahi, *Journal of the Taiwan Institute of Chemical Engineers*, 2014, **45**, 275-282.
15 A. L. Ahmad, B. S. Ooi, A. W. Mohammad and J. P. Choudhury, *Industrial & Engineering Chemistry Research*, 2004, **43**, 8074-8082.
16 N. K. Saha and S. V. Joshi, *Journal of Membrane Science*, 2009, **342**, 60-69.
17 P. G. Ingole, H. C. Bajaj and K. Singh, *Desalination*, 2012, **305**, 54-63.
18 P. G. Ingole, K. Singh and H.C. Bajaj, *Indian Journal of Chemical Technology*, 2011, **18**, 197-206.
19 S. H. Yun, P. G. Ingole, K. H. Kim, W. K. Choi, J. H. Kim and H. K. Lee, *Chemical Engineering Journal*, 2014, **258**, 348-356.
20 A. P. Rao, S. V. Joshi, J. J. Trivedi, C. V. Devmurari and V. J. Shah, *Journal of Membrane Science*, 2003, **211**, 13-24.
21 M. Oldani and G. Shock, *Journal of Membrane Science*, 1989, **43**, 243-258.
22 Y. Jin and Z. Su, *Journal of Membrane Science*, 2009, **330**, 175-179.
23 Z.-Y. Xi, Y.-Y. Xu, L. P. Zhu, Y. Wang and B.-K. Zhu, *Journal of Membrane Science*, 2009, **327**, 244-253.
24 G. Beamson and D. Briggs, *Willey Interscience*, 1992.
25 S. J. Park, J. S. Hwang, W. K. Choi, H. K. Lee and K. M. Huh, *Polymer (Korea)*, 2013, **38**, 205-212.
26 R. R. Pawar, B. D. Kevadiya, H. Brahmbhatt and H. C. Bajaj, *International Journal of Pharmaceutics*, 2013, **446,** 145-152.
27 A. Vesel, I. Junkar, U. Cvelbar, J. Kovac and M. Mozetic, *Surface and Interface Analysis*, 2008, DOI: 10.1002/sla.2923.
28 W. Lihong, L. Deling, C. Lihua, Z. Lin and C. Hualin, *Chinese Journal of Chemical Engineering*, 2011, **19**, 262-266.
29 L.M. Robeson, *Journal of Membrane Science*, 1991, **62**, 165–185.

